

Anisotropic Superexchange for nearest and next nearest coppers in chain, ladder and lamellar cuprates

Sabine Tornow, O. Entin-Wohlman and Amnon Aharony

School of Physics and Astronomy, Raymond and Beverly Sackler Faculty of Exact Sciences,

Tel Aviv University, Tel Aviv 69978, Israel

(July 8, 2021)

We present a detailed calculation of the magnetic couplings between nearest-neighbor and next-nearest-neighbor coppers in the edge-sharing geometry, ubiquitous in many cuprates. In this geometry, the interaction between nearest neighbor coppers is mediated via two oxygens, and the Cu–O–Cu angle is close to 90° . The derivation is based on a perturbation expansion of a general Hubbard Hamiltonian, and produces numerical estimates for the various magnetic energies. In particular we find the dependence of the anisotropy energies on the angular deviation away from the 90° geometry of the Cu–O–Cu bonds. Our results are required for the correct analysis of the magnetic structure of various chain, ladder and lamellar cuprates.

I. INTRODUCTION

The magnetic interactions in the copper oxides are believed to be governed by kinetic superexchange through the intervening oxygens. In tetragonal symmetry, one may view the CuO planes as consisting of clusters of four oxygens, forming a square whose center is occupied by a copper ion. These squares can be lined up along their edges, and then the nearest neighbor (NN) Cu–O–Cu bond makes an almost 90° angle. Another ubiquitous configuration is formed when the squares are connected along their corners, in which case the nearest neighbor Cu–O–Cu bond is linear, having an angle of 180° . Typical examples for edge-sharing compounds are $\text{La}_6\text{Ca}_8\text{Cu}_{24}\text{O}_{41}$ ¹ (where the angle is 91°) and CuGeO_3 (where the angle is $\approx 98^\circ$).² Corner-sharing configurations characterize the copper oxide planes in the parent compounds of the high- T_c cuprates, and the chains in Sr_2CuO_3 ³ and SrCuO_2 .⁴ Some compounds include both types of bonds, for example $\text{Sr}_2\text{Cu}_3\text{O}_4\text{Cl}_2$.⁵ The various Cu–Cu bond geometries in this material are the same as those for the nearest-neighbors and next-nearest-neighbors (NNN) in the chains in $\text{Sr}_{14}\text{Cu}_{24}\text{O}_{41}$ ⁶ and the interladder bonds in $\text{Sr}_{n-1}\text{Cu}_{n+1}\text{O}_{2n}$.⁷

The magnitude and the sign of the magnetic interactions in the two types of bonds are expected to be quite different. According to the so-called Goodenough–Kanamori–Anderson (GKA) rules,⁸ the *leading* isotropic superexchange of a 180° bond between two magnetic ions with partially filled d shells is strongly antiferromagnetic, while the leading order of a 90° superexchange is ferromagnetic, and much weaker. In the Cu–O case, the reason for this is that for the corner-sharing geometry, the $2p_\sigma$ orbital hybridizes with the two neighboring Cu ions, yielding a significant contribution to the kinetic superexchange (which is antiferromagnetic). In contrast, in the edge-sharing configuration the $2p_\sigma$ orbital on the oxygen, which hybridizes with a 3d orbital on one copper, is almost orthogonal to that 3d orbital on the nearest-neighbor Cu ion, thus blocking the antiferromagnetic superexchange via a single oxygen. The leading magnetic

coupling in this case is given by the next order perturbation terms, and is therefore weaker and of the opposite sign.

Higher-order perturbation terms also determine the magnetic *anisotropies*, in both types of bonds. These anisotropies are responsible for various observable quantities, like the gaps in the spin wave spectrum, the spin orientations in space, etc, and hence are of much interest. The magnetic couplings of the linear Cu–O–Cu bond were investigated in great detail (see Refs. 9 and 10 and references therein), yielding the in-plane and the out-of-plane gaps of the family of compounds with structures similar to that of La_2CuO_4 , as well as the antisymmetric Dzyaloshinskii–Moriya interaction in the orthorhombic phase. In particular, the role of the on-site Coulomb exchange and the spin-orbit interaction in producing the various anisotropies was clarified in tetragonal and orthorhombic symmetries.

In the almost- 90° bond (see Fig. 1) the leading order magnetic exchange is small. Therefore, higher-order perturbation processes, as well as details of the structure like the presence of side groups^{11,12} have a significant contribution. For the same reason, next-nearest-neighbor Cu–Cu couplings are expected to be much more important than in the case of the linear Cu–Cu bond configuration.

Previous discussions of this geometry include an analysis of the dependence of the leading nearest-neighbor *isotropic* coupling on the small angular deviation away from 90° , δ ,^{11–15} which has been found to be dominated by the on-site Coulomb exchange interaction on the oxygens,¹³ and the non-local exchange between the coppers and the oxygens.^{11,12} The magnetic *anisotropies* have been calculated only for the nearest-neighbor, strictly 90° -bond, by Yushankhai and Hayn.¹⁶ We compare below their results with ours.

The aim of this paper is to present a detailed calculation of both the isotropic and the anisotropic magnetic interactions in the nearly- 90° configuration shown in Fig. 1, for nearest-neighbor and next-nearest-neighbor copper ions. Our calculation is based on the perturbation expansion of a Hubbard model around the half-filled ground

state, in which there is a single 3d hole on each copper ion, and the oxygen 2p states are completely full. Since the spin of the Cu hole is arbitrary, this ground state is 2^N -fold degenerate, where N is the number of copper ions. The superexchange magnetic Hamiltonian is obtained as the effective interaction within this degenerate manifold. The microscopic Hamiltonian we consider includes hopping between all orbitals on the copper d-states and on the oxygen p-states, and between the p states on neighboring oxygens. The Hamiltonian also contains the spin-orbit interactions on the copper. Those on the oxygen are much weaker and are therefore neglected. We also include all local Coulomb interactions on the copper and on the oxygen, and the non-local Coulomb exchange between the copper and the oxygen.

General expressions for the effective magnetic Hamiltonian, based on this microscopic Hamiltonian have been derived before.^{9,10} In order to keep the paper self-contained we reproduce in Sec. II the main steps of the derivation. We find in Sec. II that the magnetic Hamiltonian has the form

$$\mathcal{H} = \sum_{\langle ij \rangle} \sum_{\mu} (J_{NN}^{\mu} S_i^{\mu} S_j^{\mu} + J_{NNN}^{\mu} S_i^{\mu} S_j^{\mu}), \quad (1)$$

in which μ denotes the Cartesian component of the spin and J_{NN} and J_{NNN} are the magnetic couplings between nearest-neighbors and next-nearest-neighbors, respectively. It is convenient to define the coordinate system for the spin components such that the x and y directions are in the Cu–O plane, along the bonds between the copper, and the z direction is perpendicular to the plane. The leading magnetic coupling for both NN and NNN is

$$J^{av} = \frac{J^x + J^y + J^z}{3}. \quad (2)$$

The anisotropic couplings are then naturally given by J^{op} , for the out-of-plane anisotropy, and J^{pd} , for the in-plane one:

$$J^{op} = J^z - \frac{J^x + J^y}{2}, \quad J^{pd} = \frac{J^x - J^y}{2}. \quad (3)$$

(The notation “pd” stands for pseudo-dipolar, see Ref. 7.)

The parameters that determine the magnitude and the sign of the magnetic couplings are the Cu–O and O–O hopping matrix elements, the on-site (single particle) energies on the oxygen and on the copper, the spin-orbit coupling constant λ and the various Coulomb matrix elements. The latter are parametrized¹⁷ in terms of the Racah parameters into the on-site leading order interactions, and the residual remaining interactions, which are small. However, they, as well as λ , are necessary for the generation of the magnetic anisotropies. All these parameters depend on the crystal symmetry, and hence on the angle δ (see Fig. 1). Adopting the plausible assumption that the most important sensitivity to small deviations

from 90° occurs in the Cu–O hopping matrix elements, we have included only their dependence on the angle,¹⁸ and calculated the angular dependence of the magnetic interactions for small angles δ . The explicit expressions for the magnetic couplings are given in Secs. III and IV. Here we summarize the results, which are depicted in Fig. 2 for the nearest-neighbor couplings, and in Fig. 3 for the next-nearest-neighbor ones.

The numerical estimates are computed using the following parameters. We take the on-site energies on the oxygen to be $\epsilon_{p_x} = \epsilon_{p_y} = 3\text{eV}$ and $\epsilon_{p_z} = 2\text{eV}$.¹⁰ Those on the copper are assumed for simplicity to be identical, $\epsilon_{\alpha} = 1.8\text{eV}$ ($\alpha = 0, 1, x, y, z$, see definitions below).⁹ The spin-orbit coupling on the copper is taken to be $\lambda = 0.1\text{eV}$. The on-site Coulomb matrix elements necessitate the Racah parameters A , B , and C for the copper, and F_0 and F_2 on the oxygen.^{9,10} These are chosen as $A = 7.0\text{eV}$, $B = 0.15\text{eV}$, $C = 0.58\text{eV}$, $F_0 = 3.1\text{eV}$, and $F_2 = 0.28\text{eV}$. There is no reliable estimate for the non-local Coulomb exchange between the copper and the oxygen.^{11,12,14} We therefore take as a representative estimate a value in the range between 0.02eV and 0.1eV.^{11,12,14}

The hopping matrix elements can be expressed in terms of the Slater–Koster parameters,¹⁸ $t_0 = -\sqrt{3}(pd\sigma)/2$, $t_1 = -(pd\sigma)/2$, and $t_2 = (pd\pi)$, for the Cu–O ones, and $t_3 = (1/2)((pp\sigma) + (pp\pi))$, $t_4 = (1/2)((pp\sigma) - (pp\pi))$, and $t_5 = (pp\pi)$ for the O–O matrix elements. We have used the values $(pd\sigma) = 1.5\text{eV}$,^{9,10} and $(pp\pi) = -0.6\text{eV}$,¹⁹ and used the relations $(pp\pi) = -\frac{1}{4}(pp\sigma)$ and $(pd\pi) = -\frac{1}{2}(pd\sigma)$.²⁰

Figure 2 depicts the angular dependence of J_{NN}^{av} , J_{NN}^{op} , and J_{NN}^{pd} . The three curves in each figure are obtained by choosing different representative values for the non-local Cu–O Coulomb exchange matrix element, K . At strictly 90°, J_{NN}^{av} is negative (ferromagnetic) and small, $\approx -0.02\text{eV}$ (-0.04eV , -0.07eV) for $K = 0.02\text{eV}$ (0.05eV , 0.1eV). Its value is determined mainly by the residual Coulomb interactions. As the angle deviates from 90°, J_{NN}^{av} approaches zero and changes its sign at about $\delta \approx 0.05$ (0.065 , 0.09) (2.9° , 3.7° , 5.2°). These results agree with those found before in Refs. 12 and 14. The out-of-plane anisotropy J_{NN}^{op} is relatively large, and negative, in agreement with the findings of Ref. 16. Like all other anisotropies, its magnitude is proportional to λ^2 . However, for delicate reasons related to “ring-exchange” processes (see below), the Coulomb matrix element that scales its magnitude is the on-site interaction on the oxygen, leading to its comparatively high value, $\approx -1.3\text{meV}$ at 90°. (The out-of-plane anisotropy increases slightly with increasing K .) The nearest-neighbor in-plane anisotropy J_{NN}^{pd} is scaled by the small residual Coulomb interactions. It vanishes at $\delta = 0$, and stays quite small away from that value, varying approximately linearly with δ , $\approx (-0.1 \text{ to } -1.7 K)\delta \text{ meV}$.

The case of an ideal 90° nearest-neighbor bond has been recently discussed in Ref. 16. These authors have

specialized to materials of the type $A_2Cu_3O_4Cl_2$, with $A=$ Ba or Sr. They have neglected the non-constant on-site Coulomb interactions on the oxygen and the non-local Cu–O Coulomb interaction, but have taken into account the local orthorhombic symmetry, by allowing the Cu on-site energies ϵ_x and ϵ_y to be different. They therefore obtained a small in-plane anisotropy, of the order of $0.2\mu\text{eV}$.

The analogous results for the next-nearest-neighbor couplings are summarized in Fig. 3. These necessitate additional perturbation processes, which involve hopping between nearest-neighbor oxygens. We find that $J_{\text{NNN}}^{\text{av}}$ is about 20meV at 90° , and has a smooth linear dependence on δ away from it, remaining antiferromagnetic for small angles, in agreement with the findings of Refs. 12 and 14.

As in the case of the nearest neighbors, also the anisotropic coupling $J_{\text{NNN}}^{\text{op}}$ is relatively large and negative, being $\approx -0.036\text{meV}$ at 90° , while $J_{\text{NNN}}^{\text{pd}}$ is extremely minute, $\approx -6\mu\text{eV}$. The out-of-plane anisotropy is again dominated by the “ring-exchange” processes and the in-plane anisotropy by the small residual Coulomb interactions ΔU .

Obviously, the results summarized in Figs. 2 and 3 depend on the details of the parameters, e.g., the hopping matrix elements or the Coulomb Racah coefficients. The remaining Sections of the paper are devoted to a detailed discussion of the derivation and the choice of these parameters.

II. THE MAGNETIC HAMILTONIAN

As is discussed above, the magnetic Hamiltonian is derived from a microscopic Hamiltonian. The latter can be written as follows:

$$\mathcal{H} = \mathcal{H}_{Cu} + \mathcal{H}_O + \mathcal{H}_{Cu-O}, \quad (4)$$

with obvious notations. Explicitly, the Cu-ion Hamiltonian is

$$\begin{aligned} \mathcal{H}_{Cu} = & \sum_{i\alpha\sigma} \epsilon_\alpha d_{i\alpha\sigma}^\dagger d_{i\alpha\sigma} + \frac{\lambda}{2} \sum_{\substack{i\alpha\beta \\ \sigma\sigma'}} \mathbf{L}_{\alpha\beta} \cdot [\sigma]_{\sigma\sigma'} d_{i\alpha\sigma}^\dagger d_{i\beta\sigma'} \\ & + \frac{1}{2} \sum_{\substack{i\sigma\sigma' \\ \alpha\beta\gamma\delta}} U_{\alpha\beta\gamma\delta} d_{i\alpha\sigma}^\dagger d_{i\beta\sigma'}^\dagger d_{i\gamma\sigma'} d_{i\delta\sigma}, \end{aligned} \quad (5)$$

where $d_{i\alpha\sigma}^\dagger$ creates a hole with spin σ in the crystal-field state α at site i , of site energy ϵ_α . For tetragonal symmetry we label the crystal-field states as $|0\rangle \sim x^2 - y^2$, $|1\rangle \sim 3z^2 - r^2$, $|z\rangle \sim xy$, $|x\rangle \sim yz$, and $|y\rangle \sim zx$, where the z axis is perpendicular to the plane and $|0\rangle$ is the lowest energy single-particle state. The second term in (5) is the spin-orbit interaction, where λ is the spin-orbit coupling constant and $\mathbf{L}_{\alpha\beta}$ denotes the matrix elements of the

orbital angular momentum vector between the crystal-field states α and β . The non-zero matrix elements are $L_{0z}^z = -2i$, $L_{0x}^x = L_{0y}^y = i$, $L_{1x}^x = -L_{1y}^y = \sqrt{3}i$, $L_{zx}^y = -L_{zy}^x = L_{xy}^z = i$, and $L_{\alpha\beta}^* = L_{\beta\alpha}$. The last term in (5) is the Coulomb interaction, with $U_{\alpha\beta\gamma\delta} = \langle \alpha\delta | \beta\gamma \rangle$ in the notations of Table A26 in Ref. 17. The Hamiltonian of the oxygen ions is

$$\begin{aligned} \mathcal{H}_O = & \sum_{qn\sigma} \epsilon_n p_{qn\sigma}^\dagger p_{qn\sigma} + \sum_{\substack{mn\sigma \\ qq'}} (t_{nm}^{qq'} p_{qn\sigma}^\dagger p_{q'm\sigma} + hc) \\ & + \frac{1}{2} \sum_{\substack{q\sigma\sigma' \\ n_1 n_2 n_3 n_4}} U_{n_1 n_2 n_3 n_4} p_{qn_1\sigma}^\dagger p_{qn_2\sigma'}^\dagger p_{qn_3\sigma'} p_{qn_4\sigma}, \end{aligned} \quad (6)$$

in which $p_{qn\sigma}^\dagger$ creates a hole in one of the three p orbitals, p_x , p_y , and p_z (denoted by n) on the oxygen at site q , with energy ϵ_n . The second term in (6) describes the hopping between the O-ions, and the last term is the Coulomb interaction on the O-ions. Finally, \mathcal{H}_{Cu-O} describes the kinetic energy of hopping between the Cu and the O ions, and the Coulomb exchange interaction between them,

$$\begin{aligned} \mathcal{H}_{Cu-O} = & \sum_{\substack{iq\sigma \\ \alpha\alpha n}} (t_{n\alpha}^{qi} p_{qn\sigma}^\dagger d_{i\alpha\sigma} + hc) \\ & + \sum_{\substack{iq\sigma\sigma' \\ \alpha\beta mn}} K_{\alpha m \beta n} d_{i\alpha\sigma}^\dagger p_{qm\sigma'}^\dagger d_{i\beta\sigma'} p_{qn\sigma}. \end{aligned} \quad (7)$$

A significant simplification of the perturbation expansion is achieved by first treating the spin-orbit interactions exactly, leaving the expansion in orders of the spin-orbit coupling, λ , to the final stage.⁹ This is accomplished by introducing the unitary transformation which diagonalizes the single-particle part of \mathcal{H}_{Cu}

$$d_{i\alpha\sigma}^\dagger = \sum_{a\sigma'} [m_{\alpha a}]_{\sigma\sigma'}^* c_{ia\sigma'}^\dagger, \quad (8)$$

where $c_{ia\sigma}^\dagger$ creates a hole in the exact eigenstate a of the Hamiltonian which consists of the crystal-field and the spin-orbit interaction on the copper. These states have a site label i , a state label a , and a pseudo-spin index σ . One then has

$$\begin{aligned} \sum_{i\alpha\sigma} \epsilon_\alpha d_{i\alpha\sigma}^\dagger d_{i\alpha\sigma} + \frac{\lambda}{2} \sum_{\substack{i\alpha\beta \\ \sigma\sigma'}} \mathbf{L}_{\alpha\beta} \cdot [\sigma]_{\sigma\sigma'} d_{i\alpha\sigma}^\dagger d_{i\beta\sigma'} \\ = \sum_{ia\sigma} E_a c_{ia\sigma}^\dagger c_{ia\sigma}, \end{aligned} \quad (9)$$

where E_a and $[m_{\alpha a}]_{\sigma\sigma'}$ are determined by

$$\begin{aligned} E_b [m_{\gamma b}]_{\sigma\sigma'} = & \epsilon_\gamma [m_{\gamma b}]_{\sigma\sigma'} \\ & + \frac{\lambda}{2} \sum_{\beta\sigma_1} \mathbf{L}_{\gamma\beta} \cdot [\sigma]_{\sigma\sigma_1} [m_{\beta b}]_{\sigma_1\sigma'}, \end{aligned} \quad (10)$$

with $[\sum_a \mathbf{m}_{\beta a}(\mathbf{m}_{\alpha a})^\dagger]_{\sigma\sigma'} = \delta_{\alpha\beta}\delta_{\sigma\sigma'}$. When $\lambda \rightarrow 0$, each state $|a\rangle$ approaches one of the states $|\alpha\rangle$. Using this definition, the index a runs over the values 0, 1, z , x , and y . A detailed discussion of this transformation is given in Ref. 9.

To apply the perturbation expansion, we divide the Hamiltonian \mathcal{H} into an unperturbed part, \mathcal{H}_0 , and a perturbation term \mathcal{H}_1 . The part \mathcal{H}_0 contains the single-particle Hamiltonians on the coppers and on the oxygens, and the leading on-site Coulomb potentials. The perturbation Hamiltonian contains the kinetic energy and the residual Coulomb interactions. As is known,¹⁷ the on-site Coulomb interactions can be parametrized in terms of the Racah coefficients. In tetragonal site symmetry, those on the copper are parametrized by the Racah parameters A , B , and C , with $A \gg B$ and $A \gg C$, and those on the oxygen by F_0 and F_2 , with $F_0 \gg F_2$. We choose the on-site leading Coulomb interactions to be $U_0 \equiv U_{\alpha\alpha\alpha\alpha} = A + 4B + 3C$ for the copper, and $U_q \equiv U_{nnnn} = F_0 + 4F_2$ on the oxygen. Consequently, the unperturbed Hamiltonian is

$$\begin{aligned} \mathcal{H}_0 = & \sum_{ia\sigma} E_a c_{ia\sigma}^\dagger c_{ia\sigma} + \frac{U_0}{2} \sum_{\substack{iab \\ \sigma\sigma'}} c_{ia\sigma}^\dagger c_{ib\sigma'}^\dagger c_{ib\sigma'} c_{ia\sigma} \\ & + \sum_{qn\sigma} \epsilon_n p_{qn\sigma}^\dagger p_{qn\sigma} + \frac{U_q}{2} \sum_{\substack{qnn' \\ \sigma\sigma'}} p_{qn\sigma}^\dagger p_{qn'\sigma'}^\dagger p_{qn'\sigma'} p_{qn\sigma}. \end{aligned} \quad (11)$$

The perturbation Hamiltonian is

$$\mathcal{H}_1 = \mathcal{H}_{hop} + \Delta\mathcal{H}_C, \quad (12)$$

in which the hopping term is

$$\begin{aligned} \mathcal{H}_{hop} = & \sum_{\substack{igan \\ \sigma\sigma'}} (\tilde{t}_{an}^{iq})_{\sigma'\sigma} c_{ia\sigma}^\dagger p_{qn\sigma} + hc \\ & + \sum_{\substack{nms \\ qq'}} (t_{nm}^{qq'})_{\sigma\sigma'}^\dagger p_{qn\sigma} p_{q'm\sigma} + hc. \end{aligned} \quad (13)$$

Because of the transformation (8), the Cu–O hopping becomes spin-dependent

$$[\tilde{t}_{an}^{iq}]_{\sigma'\sigma} = \sum_{\alpha} t_{\alpha n}^{iq} [m_{\alpha a}]_{\sigma\sigma'}^*. \quad (14)$$

The term $\Delta\mathcal{H}_C$ contains the (small) additional on-site Coulomb interactions, and the non-local Cu–O Coulomb potential,

$$\begin{aligned} \Delta\mathcal{H}_C = & \frac{1}{2} \sum_{\substack{iabcd \\ s_1s_2s_3s_4}} \Delta U_{s_1s_2s_3s_4}(abcd) c_{ias_1}^\dagger c_{ib}s_2^\dagger c_{ics_3} c_{ids_4} \\ & + \frac{1}{2} \sum_{\substack{q\sigma\sigma' \\ n_1n_2n_3n_4}} \Delta U_{n_1n_2n_3n_4} p_{qn_1\sigma}^\dagger p_{qn_2\sigma'}^\dagger p_{qn_3\sigma'} p_{qn_4\sigma} \\ & + \sum_{\substack{iqabmn \\ ss'\sigma\sigma'}} K_{ss'\sigma\sigma'}(ambn) c_{ias}^\dagger p_{qmn\sigma'}^\dagger c_{ib}s' p_{qn\sigma}, \end{aligned} \quad (15)$$

with

$$\begin{aligned} & \Delta U_{s_1s_2s_3s_4}(abcd) \\ & = \sum_{\alpha\beta\gamma\delta} \Delta U_{\alpha\beta\gamma\delta} [(\mathbf{m}_{\alpha a})^\dagger \mathbf{m}_{\delta d}]_{s_1s_4} [(\mathbf{m}_{\beta b})^\dagger \mathbf{m}_{\gamma c}]_{s_2s_3}, \end{aligned} \quad (16)$$

and

$$K_{ss'\sigma\sigma'}(ambn) = \sum_{\alpha\beta} K_{\alpha m\beta n} [m_{\alpha a}]_{\sigma s}^* [m_{\beta b}]_{\sigma' s'}. \quad (17)$$

Here we have defined $\Delta U_{\alpha\beta\beta\alpha} = U_{\alpha\beta\beta\alpha} - U_0$ and $\Delta U_{nn'n'n} = U_{nn'n'n} - U_q$. For $\alpha \neq \delta$ or $\beta \neq \gamma$, and $n_1 \neq n_4$ or $n_2 \neq n_3$, $\Delta U \equiv U$ involves only the small Racah coefficients B , C , and F_2 .¹⁷

All the perturbation contributions resulting from \mathcal{H}_1 begin and end within the 2^N -fold degenerate ground-state manifold of \mathcal{H}_0 , each state of which has one hole at each copper site, with arbitrary spin σ . We will denote by “0” the ground state of the single-particle Hamiltonian on the copper, and will take its site energy to be zero. For the sake of clarity, we divide the perturbation channels into three groups. Group “a” includes the processes in which there are two holes on the copper in the intermediate step; group “b” includes those in which there are two holes on the oxygen in the intermediate step, or processes where the two holes exchange their corresponding coppers by going around the ring formed by the two coppers and the intervening oxygen (for example, coppers i and j , and oxygens q and q' in Fig. 4); group “c” contains the contribution from the non-local Coulomb exchange between the coppers and the oxygens.²¹

The contribution of channel “a” to the magnetic coupling of coppers i and j is

$$\begin{aligned} \mathcal{H}_a(i, j) = & \frac{1}{U_0} Tr \left\{ \sigma \cdot \mathbf{S}_i \tilde{\mathcal{T}}_{00}^{ij} \sigma \cdot \mathbf{S}_j \tilde{\mathcal{T}}_{00}^{ji} \right\} \\ & + \sum_{\substack{ab \\ \alpha\beta\gamma\delta}} \frac{\Delta U_{\alpha\beta\gamma\delta}}{(U_0 + E_a)(U_0 + E_b)} \times \\ & \left(Tr \left\{ \sigma \cdot \mathbf{S}_i \tilde{\mathcal{T}}_{0b}^{ij} (\mathbf{m}_{\alpha b})^\dagger \mathbf{m}_{\delta a} \tilde{\mathcal{T}}_{a0}^{ji} \right\} Tr \left\{ \sigma \cdot \mathbf{S}_j (\mathbf{m}_{\beta 0})^\dagger \mathbf{m}_{\gamma 0} \right\} \right. \\ & \left. - Tr \left\{ \sigma \cdot \mathbf{S}_i \tilde{\mathcal{T}}_{0b}^{ij} (\mathbf{m}_{\alpha b})^\dagger \mathbf{m}_{\delta 0} \sigma \cdot \mathbf{S}_j (\mathbf{m}_{\beta 0})^\dagger \mathbf{m}_{\gamma a} \tilde{\mathcal{T}}_{a0}^{ji} \right\} \right) \\ & + (i \leftrightarrow j), \end{aligned} \quad (18)$$

in which \mathbf{S}_i is the spin on the copper at site i in the new orbital ground state $|a\rangle = |0\rangle$,

$$\mathbf{S}_i = \frac{1}{2} \sum_{\sigma\sigma'} c_{i0\sigma}^\dagger [\sigma]_{\sigma\sigma'} c_{i0\sigma'}, \quad (19)$$

and the “ Tr ” are carried out in spin space.²² We have introduced in (18) the notation $\tilde{\mathcal{T}}_{ba}^{ij}$ for the effective matrix element for hopping from state a on copper j to state b on copper i . These are different in the case where the two coppers are nearest neighbors, and when they are

next-nearest neighbors. In the first case such a process can be achieved through a single oxygen, yielding

$$[\tilde{\mathcal{T}}_{ba}^{ij}]_{\sigma'\sigma} = \sum_{qn\sigma_1} \frac{1}{\epsilon_n} [\tilde{t}_{bn}^{iq}]_{\sigma'\sigma_1} [\tilde{t}_{na}^{qj}]_{\sigma_1\sigma}, \quad (20)$$

to lowest possible order in perturbation theory. Figure 4 depicts the direct hopping from copper i to oxygen q , together with the two possible indirect hoppings, going through oxygen q' and oxygen q'' . To account for these processes one has to use the following replacement in (20)

$$[\tilde{t}_{na}^{qi}]_{\sigma_1\sigma} \rightarrow [\tilde{t}_{na}^{qi}]_{\sigma_1\sigma} - \sum_{mq'} \frac{1}{\epsilon_m} t_{nm}^{qq'} [\tilde{t}_{ma}^{q'i}]_{\sigma_1\sigma}. \quad (21)$$

When the two coppers are NNN, the O–O hopping is essential for bringing the two holes to the same copper. (For example, the bond $j'-j$ in Fig. 4 requires the $q-q''$ hopping.) In this case we have

$$[\tilde{\mathcal{T}}_{ba}^{ij}]_{\sigma'\sigma} = \sum_{qn\sigma_1} \frac{1}{\epsilon_n} [\tilde{t}_{bn}^{iq}]_{\sigma'\sigma_1} [\tilde{T}_{na}^{qi}]_{\sigma_1\sigma}, \quad (22)$$

where

$$[\tilde{T}_{na}^{qi}]_{\sigma_1\sigma} = \sum_{mq'} \frac{1}{\epsilon_m} t_{nm}^{qq'} [\tilde{t}_{ma}^{q'i}]_{\sigma_1\sigma}. \quad (23)$$

The perturbation contributions coming from channel b, when coppers i and j are NN, yield

$$\begin{aligned} \mathcal{H}_b(i,j) = & \sum_{mnqq'} \left(\frac{1}{\epsilon_n} + \frac{1}{\epsilon_m} \right)^2 \times \\ & \left(\delta_{qq'} \frac{1}{\epsilon_n + \epsilon_m + U_q} + (1 - \delta_{qq'}) \frac{1}{\epsilon_n + \epsilon_m} \right) \times \\ & \text{Tr} \left\{ \sigma \cdot \mathbf{S}_i \tilde{t}_{0m}^{iq} \tilde{t}_{m0}^{qj} \sigma \cdot \mathbf{S}_j \tilde{t}_{0n}^{jq} \tilde{t}_{no}^{qi} \right\} \\ & + \sum_{\substack{qnm \\ n'm'}} \left(\frac{1}{\epsilon_n} + \frac{1}{\epsilon_{n'}} \right) \left(\frac{1}{\epsilon_m} + \frac{1}{\epsilon_{m'}} \right) \times \\ & \frac{\Delta U_{mm'nn'}}{(U_q + \epsilon_n + \epsilon_{n'})(U_q + \epsilon_m + \epsilon_{m'})} \times \\ & \left(\text{Tr} \left\{ \sigma \cdot \mathbf{S}_i \tilde{t}_{0m}^{iq} \tilde{t}_{n'0}^{qj} \right\} \text{Tr} \left\{ \sigma \cdot \mathbf{S}_j \tilde{t}_{0m'}^{jq} \tilde{t}_{n0}^{qi} \right\} \right. \\ & \left. - \text{Tr} \left\{ \sigma \cdot \mathbf{S}_i \tilde{t}_{0m}^{iq} \tilde{t}_{n'0}^{qj} \sigma \cdot \mathbf{S}_j \tilde{t}_{0m'}^{jq} \tilde{t}_{n0}^{qi} \right\} \right). \end{aligned} \quad (24)$$

The term with the $(1 - \delta_{qq'})$ in front arises in the chain geometry and does not have the on-site Coulomb interaction in the denominator.^{11,23} As non-local Coulomb interactions between the oxygens are ignored here, there is no analogous contribution in the second sum of (24). When the two coppers are NNN, one must invoke the O–O hopping. We then find that each pair of matrix elements \tilde{t} has to be replaced as follows

$$\tilde{t}^{qi} \tilde{t}^{qj} \rightarrow -\tilde{T}^{qi} \tilde{t}^{qj} - \tilde{t}^{qi} \tilde{T}^{qj}, \quad (25)$$

where both \tilde{t} and \tilde{T} are matrices in spin space, given by Eqs. (14) and (23), respectively.

Finally, channel c gives

$$\begin{aligned} \mathcal{H}_c(i,j) = & - \sum_{\substack{qmn \\ \alpha\gamma}} \frac{K_{\alpha m \gamma n}}{\epsilon_n \epsilon_m} \text{Tr} \left\{ \sigma \cdot \mathbf{S}_i (\mathbf{m}_{\alpha 0})^\dagger \tilde{t}_{n0}^{qj} \sigma \cdot \mathbf{S}_j \tilde{t}_{0m}^{jq} \mathbf{m}_{\gamma 0} \right\} \\ & + (i \leftrightarrow j), \end{aligned} \quad (26)$$

when the two coppers are NN. The corresponding expression for NNN coppers is obtained from (26) by replacing each matrix element \tilde{t} by \tilde{T} .

The total effective magnetic interaction is the sum of the three groups. This is now expanded up to second order in the spin-orbit coupling λ . This requires the matrix m , Eq. (8), up to first order in λ only. Using Eq. (10) we have

$$[m_{\alpha a}]_{\sigma\sigma'} = \delta_{\alpha a} \delta_{\sigma\sigma'} - \frac{\lambda \mathbf{L}_{\alpha a} \cdot [\sigma]_{\sigma\sigma'}}{2(\epsilon_\alpha - E_a)}. \quad (27)$$

A further significant simplification of the expressions is achieved when one takes into account the symmetry properties of the Coulomb matrix elements:^{9,10} $\Delta U_{\alpha\beta\gamma\delta}$ vanishes unless the values of α , β , γ , and δ are such that the products $\sigma(\alpha)\sigma(\delta)$ and $\sigma(\beta)\sigma(\gamma)$ are proportional to each other. Here we use the convention that $\sigma(\alpha = 0)$ and $\sigma(\alpha = 1)$ are the unit matrix. Similarly, the non-vanishing matrix elements of $\Delta U_{n_1 n_2 n_3 n_4}$ satisfy $\sigma(n_1)\sigma(n_4) \propto \sigma(n_2)\sigma(n_3)$, and those of $K_{\alpha m \beta n}$ vanish unless $\sigma(\alpha)\sigma(n) \propto \sigma(\beta)\sigma(m)$.

In the following we present the general expressions in the form

$$\mathcal{H}(i,j) = \left(J - \frac{1}{2} \text{Tr} \mathbf{\Gamma} \right) \mathbf{S}_i \cdot \mathbf{S}_j + \mathbf{S}_i \mathbf{\Gamma} \mathbf{S}_j, \quad (28)$$

where J includes all contributions to zeroth order in λ , while the matrix $\mathbf{\Gamma}$ contains the contributions which necessitate the spin-orbit interaction, and is therefore second-order in λ . The application of these general expressions to the specific Cu–Cu bonds will be carried out in the next Section.

(a) Channel a [Eq. (18)] yields

$$J_a = 4 \left(\frac{\tilde{t}_{00}^{ij} \tilde{t}_{00}^{ji}}{U_0} - \sum_\alpha \frac{\Delta U_{\alpha 0 \alpha 0} \tilde{t}_{0\alpha}^{ij} \tilde{t}_{\alpha 0}^{ji}}{(U_0 + \epsilon_\alpha)^2} \right), \quad (29)$$

and

$$\begin{aligned} \Gamma_a^{\mu\nu} = & \frac{\lambda^2}{2U_0} \frac{L_{\mu 0}^\mu L_{\nu 0}^\nu}{\epsilon_\mu \epsilon_\nu} \times \\ & \left(\left[(t_{0\mu}^{ij} - t_{\mu 0}^{ij})(t_{0\nu}^{ji} - t_{\nu 0}^{ji}) + \mu \leftrightarrow \nu \right] + j \leftrightarrow i \right) \\ & - \frac{\lambda^2}{2} \sum_{\alpha\beta\gamma\delta} \frac{\Delta U_{\alpha\beta\gamma\delta}}{(U_0 + \epsilon_\alpha)(U_0 + \epsilon_\gamma)} \times \end{aligned} \quad (30)$$

$$\begin{aligned}
& \left(\delta_{\delta 0} \sum_{\alpha'} \frac{t_{0\alpha'}^{ij} L_{\alpha'\alpha}^\mu}{U_0 + \epsilon_{\alpha'}} + \frac{L_{\mu 0}^\mu}{\epsilon_\mu} (t_{0\alpha}^{ij} \delta_{\mu\delta} - t_{\mu\alpha}^{ij} \delta_{\delta 0}) \right) \times \\
& \left(\delta_{\beta 0} \sum_{\alpha'} \frac{t_{\alpha' 0}^{ji} L_{\gamma\alpha'}^\nu}{U_0 + \epsilon_{\alpha'}} + \frac{L_{\nu 0}^\nu}{\epsilon_\nu} (-t_{\gamma 0}^{ji} \delta_{\nu\beta} + t_{\gamma\nu}^{ji} \delta_{\beta 0}) \right) \\
& + (\mu \leftrightarrow \nu + j \leftrightarrow i). \tag{31}
\end{aligned}$$

(b) Channel b [Eq. (24)] yields

$$\begin{aligned}
J_b = 2 \sum_{mnqq'} & \left(\frac{1}{\epsilon_n} + \frac{1}{\epsilon_m} \right)^2 t_{0m}^{iq'} t_{m0}^{q'j} t_{0n}^{jq} t_{n0}^{qi} \times \\
& \left(\delta_{qq'} \frac{1}{\epsilon_n + \epsilon_m + U_q} + (1 - \delta_{qq'}) \frac{1}{\epsilon_n + \epsilon_m} \right) \\
& - 2 \sum_{mnq} \left(\frac{1}{\epsilon_n} + \frac{1}{\epsilon_m} \right)^2 \frac{\Delta U_{mnmn} (t_{0m}^{iq} t_{n0}^{qj})^2}{(\epsilon_n + \epsilon_m + U_q)^2} \\
& - 8 \sum_{nmq} \frac{1}{\epsilon_n \epsilon_m} \frac{\Delta U_{mmnn} t_{0m}^{iq} t_{n0}^{qj} t_{0n}^{jq} t_{n0}^{qi}}{(U_q + 2\epsilon_n)(U_q + 2\epsilon_m)}, \tag{32}
\end{aligned}$$

and

$$\begin{aligned}
\Gamma_b^{\mu\nu} = \lambda^2 & \frac{L_{\mu 0}^\mu L_{\nu 0}^\nu}{\epsilon_\mu \epsilon_\nu} \sum_{mnqq'} \left\{ \left(\frac{1}{\epsilon_n} + \frac{1}{\epsilon_m} \right)^2 \times \right. \\
& \left(\delta_{qq'} \frac{1}{\epsilon_n + \epsilon_m + U_q} + (1 - \delta_{qq'}) \frac{1}{\epsilon_n + \epsilon_m} \right) \times \\
& T_{0\mu}^{ij}(m, m, q') T_{0\nu}^{ji}(n, n, q) + \delta_{qq'} \frac{\Delta U_{mnmn}}{(\epsilon_n + \epsilon_m + U_q)^2} \times \\
& \left(T_{0\mu}^{ii}(m, n, q) T_{0\nu}^{jj}(n, m, q) - T_{0\mu}^{ij}(m, n, q) T_{0\nu}^{ji}(n, m, q) \right) \\
& + \delta_{qq'} \frac{4}{\epsilon_n \epsilon_m} \frac{\Delta U_{mmnn}}{(U_q + 2\epsilon_n)(U_q + 2\epsilon_m)} \times \\
& \left[T_{0\mu}^{ii}(m, n, q) T_{0\nu}^{jj}(m, n, q) - \frac{1}{2} \left(T_{0\mu}^{ij}(m, n, q) T_{0\nu}^{ji}(m, n, q) \right. \right. \\
& \left. \left. + T_{0\nu}^{ij}(m, n, q) T_{0\mu}^{ji}(m, n, q) \right) \right] \left. \right\}, \tag{33}
\end{aligned}$$

where we have defined

$$T_{0\mu}^{ij}(m, n, q) = t_{0m}^{iq} t_{n\mu}^{qj} - t_{\mu m}^{iq} t_{n0}^{qj}. \tag{34}$$

(c) Channel c [Eq. (26)] yields

$$J_c = -2 \sum_{nq} K_{0n0n} \frac{t_{n0}^{qj} t_{0n}^{jq}}{\epsilon_n^2} + (j \rightarrow i), \tag{35}$$

and

$$\begin{aligned}
\Gamma_c^{\mu\nu} = -\lambda^2 & \sum_{mnq} \frac{1}{\epsilon_m \epsilon_n} \frac{L_{\mu 0}^\mu L_{\nu 0}^\nu}{\epsilon_\mu \epsilon_\nu} \times \\
& \left(K_{\mu m 0 n} t_{n0}^{qj} t_{\nu m}^{jq} - K_{\mu m \nu n} t_{n0}^{qj} t_{0m}^{jq} \right. \\
& \left. + K_{0m\nu n} t_{n\mu}^{qj} t_{0m}^{jq} - K_{0m 0 n} t_{n\mu}^{qj} t_{\nu m}^{jq} + (j \rightarrow i) \right). \tag{36}
\end{aligned}$$

For simplicity, we have written the results for J and Γ , Eqs. (29–36) for the nearest-neighbor Cu–Cu bond. The analogous expressions for the next-NN bond are obtained using the replacements (23) and (25).

III. THE MAGNETIC COUPLINGS

A. The nearest-neighbor 90° bond

We list in Tables I and II the hopping matrix elements between Cu and O for the 90° configuration (see the Introduction and Fig. 4 for the notations). Using these values, we find that the leading order contributions to the magnetic couplings come from channels “b” and “c”, with

$$\begin{aligned}
J = J_b + J_c = & \\
& - \frac{16t_0^4 \Delta U_{p_x p_y p_x p_y}}{\epsilon_{p_x}^2 (2\epsilon_{p_x} + U_q)^2} - \frac{8t_0^2}{\epsilon_{p_x}^2} K_{0p_x 0p_x}. \tag{37}
\end{aligned}$$

in accordance with the GKA rules. Inserting the numerical values of the parameters, we find $J \approx -8\text{meV} - 0.67 K_{0p_x 0p_x}$. The leading order magnetic anisotropy in this case is the out-of-plane one,

$$\Gamma_{\text{leading order}}^{zz} = -\frac{64\lambda^2 t_0^2 t_2^2 U_q}{\epsilon_z^2 \epsilon_{p_x}^3 (2\epsilon_{p_x} + U_q)}, \tag{38}$$

with $\Gamma^{zz} \approx -1.3\text{meV}$. The processes yielding the latter are depicted in Fig. 5.

The remaining small anisotropies resulting from the on-site Coulomb potential on the oxygen, and from the non-local Coulomb exchange between the copper and the oxygen, are listed below. We express those in the coordinate system depicted in Fig. 5. To obtain the couplings in the coordinate system discussed in the Introduction, one has to rotate by 45°.

$$\begin{aligned}
\Delta \Gamma_a^{zz} = 32\lambda^2 & \frac{(4B + C)(t_0 t_2)^2}{\epsilon_{p_x}^2 \epsilon_z^2 (\epsilon_1 + U_0)^2}, \\
\Delta \Gamma_a^{xx} = \Delta \Gamma_a^{yy} = 2\lambda^2 & \frac{(3B + C)t_2^4}{\epsilon_{p_z}^2 \epsilon_x^2 (\epsilon_x + U_0)^2}, \\
\Delta \Gamma_b^{xx} = \Delta \Gamma_b^{yy} = -\frac{\lambda^2 t_0^2 t_2^2 3F_2}{\epsilon_x^2 (\epsilon_{p_x} + \epsilon_{p_z} + U_q)^2} & \left(\frac{1}{\epsilon_{p_z}} + \frac{1}{\epsilon_{p_x}} \right)^2, \\
\Delta \Gamma_c^{zz} = -\frac{8\lambda^2}{\epsilon_z^2 \epsilon_{p_x}^2} & \left(2t_0^2 K_{z p_x z p_x} + 2t_2^2 K_{0p_x 0p_x} \right. \\
& \left. + 4t_0 t_2 K_{z p_y 0p_x} \right), \\
\Delta \Gamma_c^{xx} = \Delta \Gamma_c^{yy} = -\frac{2\lambda^2}{\epsilon_y^2} & \left(\frac{t_0^2}{\epsilon_y^2} (K_{y p_x y p_x} + K_{y p_y y p_y}) \right. \\
& \left. + \frac{t_2^2}{\epsilon_{p_z}^2} K_{0p_z 0p_z} \right). \tag{39}
\end{aligned}$$

To obtain these results we have used the relations¹⁷ $U_{1010} = 4B + C$, $U_{x0x0} = U_{y0y0} = 3B + C$,

$\Delta U_{p_z p_y p_z p_y} = \Delta U_{p_z p_x p_z p_x} = 3F_2$, $\Delta U_{p_x p_x p_y p_y} = \Delta U_{p_x p_y p_x p_y}$, $K_{z p_y 0 p_x} = -K_{z p_x 0 p_y}$, $K_{x p_z 0 p_y} = K_{y p_z 0 p_x}$, $K_{0 p_y 0 p_y} = -K_{0 p_x 0 p_x}$, $K_{z p_x z p_x} = K_{z p_y z p_y}$. In addition, from Tables I and II, the only non-zero effective Cu–Cu hoppings are

$$t_{z1}^{ij} = t_{z1}^{ij} = \frac{2t_1 t_2}{\epsilon_{p_x}}, \quad t_{xy}^{ij} = t_{yx}^{ij} = \frac{2t_2^2}{\epsilon_{p_z}}. \quad (40)$$

Numerical estimates of these expressions yield $\Delta \Gamma_a^{zz} \approx 40 \mu\text{eV}$, $\Delta \Gamma_a^{xx} \approx 7 \mu\text{eV}$, $\Delta \Gamma_b^{xx} \approx -9 \mu\text{eV}$, $\Delta \Gamma_c^{zz} \approx -K \times 0.003$, $\Delta \Gamma_c^{xx} \approx -K \times 0.001$.

B. The next-nearest-neighbor 90° bond

Tables III and IV list the hopping matrix elements T_{an}^{iq} for a Cu–O–O–Cu process in the 90° configuration (the notations are shown in Fig. 4). In these Tables, $t_3 = t_{p_x p_x} = t_{p_y p_y}$, $t_4 = t_{p_x p_y}^{qq'} = -t_{p_x p_y}^{q'q}$, and $t_5 = t_{p_z p_z}$. The effective hopping matrix elements between two coppers,

$$\mathcal{T}_{ab}^{ij} = \sum_{qq' mn} \frac{1}{\epsilon_n \epsilon_m} t_{an}^{iq} t_{nm}^{qq'} t_{mb}^{q'j}, \quad (41)$$

which do not vanish are

$$\begin{aligned} \mathcal{T}_{00}^{ij} &= \frac{-2t_0^2 t_4}{\epsilon_{p_x}^2}, \quad \mathcal{T}_{11}^{ij} = \frac{2t_1^2 t_4}{\epsilon_{p_x}^2}, \quad \mathcal{T}_{zz}^{ij} = \frac{2t_2^2 t_4}{\epsilon_{p_x}^2}, \\ \mathcal{T}_{z1}^{ij} &= \mathcal{T}_{1z}^{ij} = \frac{4t_1 t_2 t_3}{\epsilon_{p_x}^2}, \quad \mathcal{T}_{xy}^{ij} = \mathcal{T}_{yx}^{ij} = \frac{t_2^2 t_5}{\epsilon_{p_z}^2}. \end{aligned} \quad (42)$$

As opposed to the NN-bond, in this case hopping between the ground state orbitals of NNN coppers is possible, via the two oxygen orbitals p_x and p_y , which are connected by t_4 , see Fig. 6. We find contributions to the coupling J from all three channels,

$$\begin{aligned} J &= J_a + J_b + J_c, \\ J_a &= \frac{64t_0^4 t_4^2}{\epsilon_{p_x}^4 U_0}, \\ J_b &= \frac{32t_0^4 t_4^2 (U_q + 4\epsilon_{p_x})}{\epsilon_{p_x}^5 (2\epsilon_{p_x} + U_q)} - \frac{32t_0^4 (t_4^2 + t_3^2) \Delta U_{p_x p_y p_x p_y}}{\epsilon_{p_x}^4 (2\epsilon_{p_x} + U_q)^2}, \\ J_c &= -8 \frac{K_{0 p_x 0 p_x}}{\epsilon_{p_x}^4} t_0^2 (t_3^2 + t_4^2), \end{aligned} \quad (43)$$

with $J \approx 0.02 \text{eV}$. The leading order anisotropy is the out-of-plane one, and comes mainly from channel “b”

$$\Gamma_{\text{leading order}}^{zz} = -\frac{256\lambda^2 t_0^2 t_2^2 t_3^2 U_q}{\epsilon_z^2 \epsilon_{p_x}^5 (2\epsilon_{p_x} + U_q)}, \quad (44)$$

$\Gamma_{\text{leading order}}^{zz} \approx -30 \mu\text{eV}$. The remaining non-diagonal anisotropies, calculated in the coordinate system of Fig. 6, are

$$\begin{aligned} \Delta \Gamma_a^{xy} &= -64\lambda^2 \Delta U_{x0x0} \frac{t_0^2 t_2^2 t_4 t_5}{(\epsilon_x + U_0) \epsilon_x^2 \epsilon_{p_z}^2 \epsilon_{p_x}^2}, \\ \Delta \Gamma_b^{xy} &= -16\lambda^2 \Delta U_{p_x p_x p_z p_z} \times \\ &\quad \frac{t_2^2 t_0^2 t_4 \left(t_3/\epsilon_{p_x} + t_5/\epsilon_{p_z} \right)}{\epsilon_x^2 \epsilon_{p_x}^2 \epsilon_{p_z} (2\epsilon_{p_x} + U_q) (2\epsilon_{p_z} + U_q)}, \\ \Delta \Gamma_c^{xy} &= -2 \frac{\lambda^2}{\epsilon_x^2 \epsilon_{p_x}^4} t_0^2 t_3 t_4 (K_{x p_x y p_y} + K_{x p_y y p_x}). \end{aligned} \quad (45)$$

Here $\Gamma^{xy} = \Gamma^{yx}$. As before, this coordinate system has to be rotated by 45° in order to produce the magnetic couplings in the form discussed in the Introduction. That is,

$$\Gamma^{xx} + \Gamma^{xy} \rightarrow \Gamma^{xx}, \quad \Gamma^{yy} - \Gamma^{xy} \rightarrow \Gamma^{yy}. \quad (46)$$

IV. SMALL DEVIATION FROM 90°

To calculate the magnetic couplings as function of the angle δ (see Figs. 1 and 7) we use the following forms for the hopping matrix elements

$$\begin{aligned} t_{0 p_x}^{1q} &= t_0 \cos \delta (1 - 2 \cos^2 \delta) + 2t_2 \sin \delta \cos \delta, \\ t_{0 p_y}^{1q} &= -t_0 \sin \delta (1 - 2 \cos^2 \delta) + 2t_2 \sin \delta \cos^2 \delta, \end{aligned} \quad (47)$$

$$\begin{aligned} \text{with } t_{0 p_x}^{q1} &= -t_{0 p_y}^{q2} \text{ and } t_{0 p_y}^{q1} = -t_{0 p_x}^{q2}, \\ t_{z p_x}^{1q} &= 2t_0 \sin \delta \cos^2 \delta + t_2 \sin \delta (2 \cos^2 \delta - 1), \\ t_{z p_y}^{1q} &= -2t_0 \cos \delta \sin^2 \delta + t_2 \cos \delta (2 \cos^2 \delta - 1), \end{aligned} \quad (48)$$

$$\begin{aligned} \text{with } t_{z p_x}^{q1} &= t_{z p_y}^{q2} \text{ and } t_{z p_y}^{q1} = t_{z p_x}^{q2}, \\ t_{1 p_x}^{1q} &= t_1 \cos \delta, \\ t_{1 p_x}^{1q} &= -t_1 \sin \delta, \end{aligned} \quad (49)$$

$$\begin{aligned} \text{with } t_{1 p_x}^{q1} &= t_{1 p_y}^{q2} \text{ and } t_{1 p_y}^{q1} = t_{1 p_x}^{q2}, \text{ and} \\ t_{x p_z}^{1q} &= -t_2 \sin \delta, \\ t_{y p_z}^{1q} &= t_2 \cos \delta, \end{aligned} \quad (50)$$

$$\text{with } t_{x p_z}^{q1} = t_{y p_z}^{q2}.$$

For the next-nearest neighbor hopping we need the following matrix elements:

$$\begin{aligned} T_{p_x \alpha} &= \frac{1}{\epsilon_{p_x}} (t_3 t_{p_x \alpha} + t_4 t_{p_y \alpha}), \\ T_{p_y \alpha} &= \frac{1}{\epsilon_{p_x}} (t_3 t_{p_y \alpha} + t_4 t_{p_x \alpha}), \end{aligned} \quad (51)$$

for $\alpha = 0, 1, z$, and

$$T_{p_z \alpha} = \frac{1}{\epsilon_{p_z}} t_5 t_{p_z \alpha} \quad (52)$$

for $\alpha = x, y$. The resulting explicit expressions for the magnetic couplings are very long, and we therefore skip them. Instead, we have used the results above to produce the curves in Figs. 2 and 3, to obtain the magnetic couplings as function of the angular deviation δ .

V. DISCUSSION

We have presented a detailed calculation of the magnetic interaction between nearest-neighbor and next-nearest-neighbor coppers in the edge-sharing geometry, and obtained numerical estimates for the various couplings as function of the angular deviation from 90° . These numerical estimates are crucial for the analysis of the magnetic structures of many chain, ladder and lamellar cuprates. Our calculation is based on a perturbation expansion of a general Hubbard Hamiltonian. It has been found before that for the magnetic *anisotropies* of the linear Cu–O–Cu bond, this expansion is quite reliable.⁹ On the other hand, it has been argued, (again for the 180° –bond), that perturbation theory fails to yield reasonable values for the leading magnetic *isotropic interactions*,²³ because the hopping matrix elements t are not necessarily small compared with the on-site energies. However, the almost 90° case discussed here is different, because of the appearance of the small Coulomb matrix elements in the expansion. It therefore can be expected that the perturbation expansion for the present case yields reliable estimates. Indeed, the comparison of our results for the NN isotropic energy with those obtained from exact diagonalization¹⁴ seem to support this conclusion.

Our results show that the out-of-plane anisotropy is negative, both for NN and for NNN coppers. This indicates an easy axis perpendicular to the Cu–O plane, in agreement with Ref. 16. We find that the pseudo-dipolar interaction between nearest-neighbors vanishes at strictly 90° , and is minute for a small deviation away from it. As has been shown in Ref. 16, this result is modified when one allows for a difference between the Cu on-site energies ϵ_x and ϵ_y . It seems that this should be the case in materials like $\text{Sr}_2\text{Cu}_3\text{O}_4\text{Cl}_2$, where some of the copper ions lose their local tetragonal symmetry: It has been found⁷ that experimental data on $\text{Sr}_2\text{Cu}_3\text{O}_4\text{Cl}_2$ imply a finite value for this energy. This means that the interpretation of the data necessitates the inclusion of such effects, or of dipolar interactions. In the same manner, it is expected that our numerical estimates as function of the angle δ will be useful in the analysis of other cuprates.

ACKNOWLEDGMENTS

We have benefitted from discussions with A. B. Harris. This project has been supported by a grant from the U. S.–Israel Binational Science Foundation (BSF). S. T. acknowledges the support by the Deutsche Forschungsgemeinschaft.

- ¹ S. A. Carter, B. Batlogg, R. J. Cava, J. J. Krajewski, W. F. Peck, Jr., and T. M. Rice, Phys. Rev. Lett. **77**, 1378 (1996).
- ² M. Hase, I. Terasak, and K. Uchinokura, Phys. Rev. Lett. **70**, 3651 (1993).
- ³ K. M. Kojima, Y. Fudamoto, M. Larkin, G. M. Luke, J. Merrin, B. Nachumi, Y. J. Uemura, N. Motoyama, H. Eisaki, S. Uchida, K. Yamada, Y. Endoh, S. Hosoya, B. J. Sternlieb, and G. Shirane, Phys. Rev. Lett. **55**, 1787 (1997).
- ⁴ M. Matsuda, K. Katsumata, K. M. Kojima, M. Larkin, G. M. Luke, J. Merrin, B. Nachumi, Y. J. Uemura, H. Eisaki, N. Motoyama, S. Uchida, G. Shirane, Phys. Rev. B**55**, R11 953 (1997).
- ⁵ K. Yamada, N. Suzuki, J. Akimitsu, Physica B **213 & 214**, 191 (1995).
- ⁶ M. Matsuda, T. Yoshihama, K. Kakurai, and S. Shirane, cond-mat/9808083.
- ⁷ F. C. Chou, A. Aharony, R. J. Birgeneau, O. Entin-Wohlman, M. Greven, A. B. Harris, M. A. Kastner, Y. J. Kim, D. S. Kleinberg, Y. S. Lee, and Q. Zhu, Phys. Rev. Lett. **78**, 535 (1997); A. Aharony, O. Entin-Wohlman, and A. B. Harris, in *Dynamical Properties of Unconventional Magnetic Systems*, A. T. Skjeltorp and D. Sherrington, eds., Kluwer Academic Publishers, 1998, p. 281.
- ⁸ J. B. Goodenough, Phys. Rev. **100**, 564 (1955); J. Kanamori, J. Phys. Chem. Solids **10**, 87 (1959); P. W. Anderson, Solid State Phys. **14**, 99 (1963).
- ⁹ T. Yildirim, A. B. Harris, A. Aharony, and O. Entin-Wohlman, Phys. Rev. B**52**, 10 239 (1995); O. Entin-Wohlman, A. B. Harris, and A. Aharony, Phys. Rev. B**53**, 11 661 (1996).
- ¹⁰ J. Stein, O. Entin-Wohlman, and A. Aharony, Phys. Rev. B**53**, 775 (1996); J. Stein, Phys. Rev. B**53**, 785 (1996).
- ¹¹ W. Geertsma and D. Khomskii, Phys. Rev. B**54**, 3011 (1996).
- ¹² M. Braden, G. Wilkendorf, J. Lorezana, M. Ain, G. J. McIntyre, M. Behruzi, G. Heger, G. Dhalegne, and A. Revcolevschi, Phys. Rev. B**54**, 1105 (1996).
- ¹³ S. Gopalan, T. M. Rice, and M. Sigrist, Phys. Rev. B**49**, 8901 (1994).
- ¹⁴ Y. Mizuno, T. Tohyama, S. Maekawa, T. Osafune, N. Motoyama, H. Eisaki, and S. Uchida, Phys. Rev. B**57**, 5326 (1998).
- ¹⁵ T. F. A. Müller, V. Anisimov, T. M. Rice, I. Dasgupta, and T. Saha-Dasgupta, cond-mat/9801280.
- ¹⁶ V. Yu. Yushankhai and R. Hayn, cond-mat/9902106.
- ¹⁷ J. S. Griffith, *The Theory of Transition Metal Ions* (Cambridge University Press, Cambridge, 1961).
- ¹⁸ J. C. Slater and G. F. Koster, Phys. Rev. **94**, 1498 (1954).
- ¹⁹ J. J. M. Pothuizen, R. Eder, N. T. Hien, M. Matoba, A. A. Menovsky, and G. A. Sawatzky, Phys. Rev. Lett. **78**, 717 (1997).
- ²⁰ L. F. Mattheiss, Phys. Rev. B**5**, 290 (1972).
- ²¹ E. B. Stechel and D. R. Jennison, Phys. Rev. B**38**, 4632 (1988).
- ²² In general, Eqs. (18), (24), and (26) may yield an anti-symmetric anisotropy, of the form $\mathbf{D} \cdot \mathbf{S}_i \times \mathbf{S}_j$, i.e., the Dzyaloshinskii–Moriya interaction. However, this interac-

tion does not appear in the symmetries considered in this paper.

²³ H. Eskes and J. H. Jefferson, Phys. Rev. B**48**, 9788 (1993).

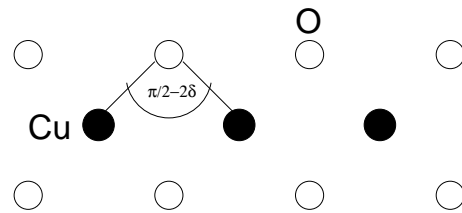


FIG. 1. Edge-sharing Cu–O configuration. The angle of the Cu–O–Cu bond is $\pi/2 - 2\delta$. Open circles denote oxygens and black circles are the Cu's.

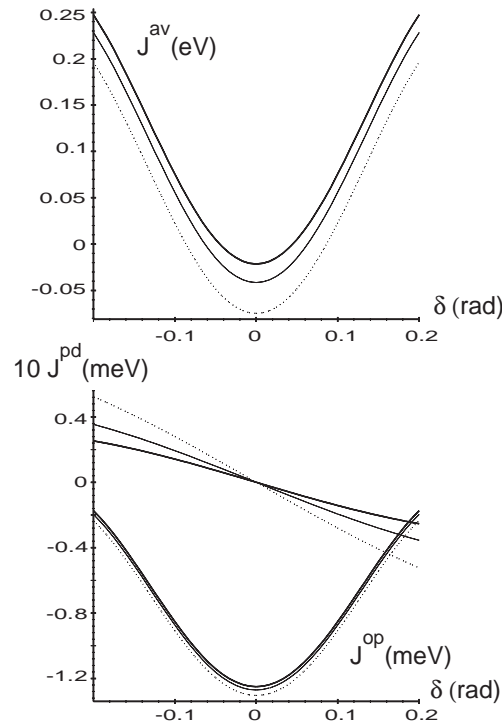


FIG. 2. The nearest-neighbor magnetic couplings J_{NN} for $K=0.02$ eV (bold solid line), $K=0.05$ eV (solid line) and $K=0.1$ eV (dashed line).

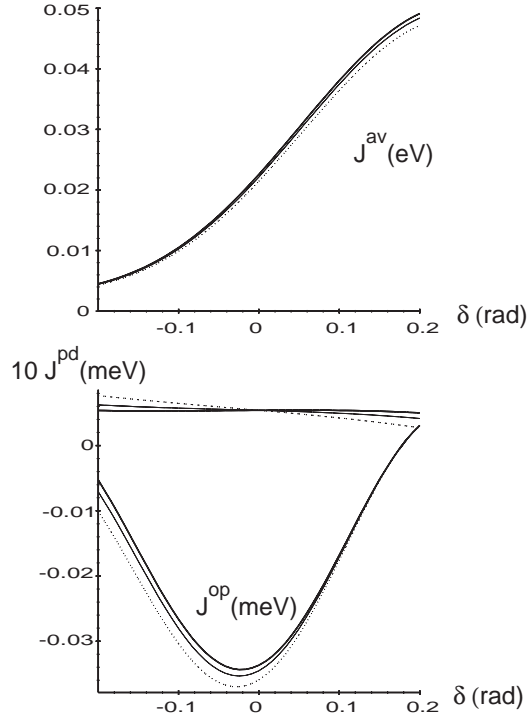


FIG. 3. The next-nearest-neighbor magnetic couplings J_{NNN} for $K=0.02$ eV (bold solid line), $K=0.05$ (solid line) and $K=0.1$ eV (dashed line).

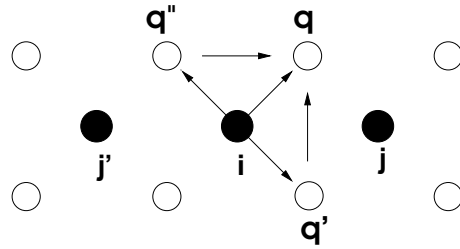


FIG. 4. The Cu–O effective nearest-neighbor hopping in the 90° bond configuration, allowing for nearest-neighbor O–O hopping. Open circles denote oxygens and black circles are the Cu's. The processes contributing to \tilde{t}^{iq} are shown by arrows.

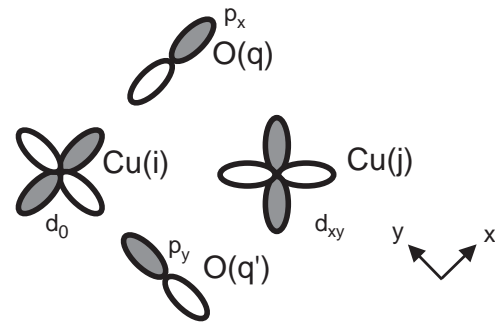


FIG. 5. Cu and O orbitals which are involved in the processes leading to the out-of-plane anisotropy Γ^{zz} . Here and below, the shaded (white) area indicates positive (negative) phase.

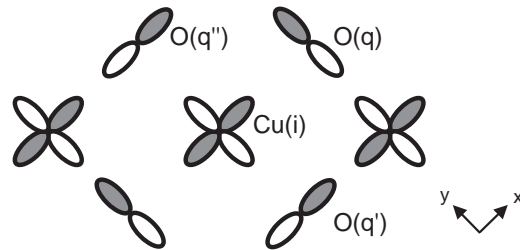


FIG. 6. Next-nearest-neighbor hopping between two $d_{x^2-y^2}$ orbitals via the p_x and p_y orbitals.

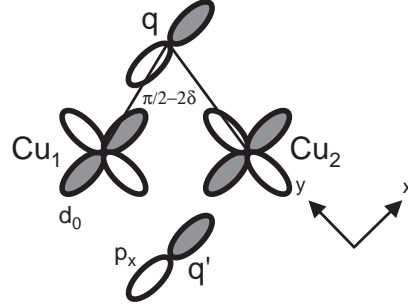


FIG. 7. Cu–O–Cu geometry for an angle $\pi/2 - 2\delta$.

TABLE I. The Cu–O hopping matrix elements $t_{\alpha n}^{iq}$ for the 90° bond. Upper signs: t^{iq} , lower signs: $t^{iq'}$.

	p_x	p_y	p_z
0	$\mp t_0$	0	0
1	$\pm t_1$	0	0
z	0	$\pm t_2$	0
x	0	0	0
y	0	0	$\pm t_2$

TABLE II. The Cu–O hopping matrix elements $t_{\alpha n}^{iq}$ for the 90° bond. Upper signs: t^{jq} , lower signs: $t^{jq'}$.

	p_x	p_y	p_z
0	0	$\pm t_0$	0
1	0	$\pm t_1$	0
z	$\pm t_2$	0	0
x	0	0	$\pm t_2$
y	0	0	0

TABLE III. The Cu–O–O hopping matrix elements $T_{\alpha n}^{iq}$ for the 90° bond. Upper signs: T^{iq} , lower signs: $T^{iq'}$.

	p_x	p_y	p_z
0	$\pm t_0 t_3 / \epsilon_{p_x}$	$\mp t_0 t_4 / \epsilon_{p_x}$	0
1	$\mp t_1 t_3 / \epsilon_{p_x}$	$\pm t_1 t_4 / \epsilon_{p_x}$	0
z	$\pm t_2 t_4 / \epsilon_{p_y}$	$\mp t_2 t_3 / \epsilon_{p_y}$	0
x	0	0	0
y	0	0	$\pm t_2 t_5 / \epsilon_{p_z}$

TABLE IV. The Cu–O–O hopping matrix elements $T_{\alpha n}^{iq}$ for the 90° bond. Upper signs: T^{jq} , lower signs: $T^{iq'}$.

	p_x	p_y	p_z
0	$\pm t_0 t_4 / \epsilon_{p_y}$	$\mp t_0 t_3 / \epsilon_{p_y}$	0
1	$\pm t_1 t_4 / \epsilon_{p_y}$	$\mp t_3 t_1 / \epsilon_{p_y}$	0
z	$\mp t_2 t_3 / \epsilon_{p_x}$	$\pm t_2 t_4 / \epsilon_{p_x}$	0
x	0	0	
y	0	0	$\pm t_2 t_5 / \epsilon_{p_z}$